COMPUTATIONAL FLUID DYNAMICS MODELING OF SOLID OXIDE FUEL CELLS

Ugur Pasaogullari and Chao-Yang Wang
Electrochemical Engine Center, and Department of Mechanical and
Nuclear Engineering, The Pennsylvania State University
University Park, PA 16802, USA

ABSTRACT

A comprehensive, multi-physics, multi-dimensional model has been developed to simulate solid oxide fuel cells (SOFC). The model fully couples electrochemical kinetics with multi-dimensional gas dynamics and multi-component transport of species. The developed model is a full cell model, including all components of SOFC, flow channels, active and inactive gas diffusion electrodes and electrolyte. The present model is implemented in a commercially available CFD software, Fluent, using its customization ability via User Defined Functions (UDF). It is able to predict conventional I-V curve (polarization curve) in addition to details of internal processes, such as flow field, species concentrations, potential and current distributions throughout the cell. It is found that mass transfer limitation plays an important role in SOFC performance, especially under high current density operation.

INTRODUCTION

Solid oxide fuel cells (SOFC) are among possible candidates of next generation energy conversion devices since they're capable of providing environmentally friendly, highly efficient power generation. Moreover, SOFCs are less sensitive to fuel composition compared to other fuel cell systems, and internal reforming of hydrocarbon fuels can be performed in-situ. This allows use of conventional hydrocarbon fuels in SOFCs without any external reformer.

Solid oxide fuel cells, like any other electrochemical device, consist of two electrodes: anode and cathode, and an electrolyte in between which allows transfer of oxygen ions. A typical SOFC operates at a temperature between 700 and 1000°C. This high operating temperature accelerates the electrochemical reaction, therefore SOFCs does not require precious metal catalysts to promote the reaction.

Planar SOFC systems have been receiving attention lately because of ease of manufacturing and higher performance compared to tubular types (1). Planar solid oxide fuel cells are generally manufactured in three different configurations according to their operating temperatures. For cells operating around 1000ºC, the electrolyte-supported cell configuration is preferred. In this design, anode and cathode are very thin (i.e. 50 μm), and the electrolyte thickness is generally larger than 100 μm. Electrolyte ionic

conductivity is a strong function of operating temperature in SOFC. For SOFC operating at lower operating temperatures, the ionic conductivity is lower, and as such anode- or cathode-supported cell configurations are preferred. In the electrode-supported cell configuration, the electrolyte is usually very thin (i.e. 20 μm), and either anode or cathode is thick enough to serve as the supporting substrate for cell fabrication. The thickness of the supporting electrode varies between 0.3 mm and 1.5 mm, depending on the design. These three planar SOFC designs are sketched in Figure 1.
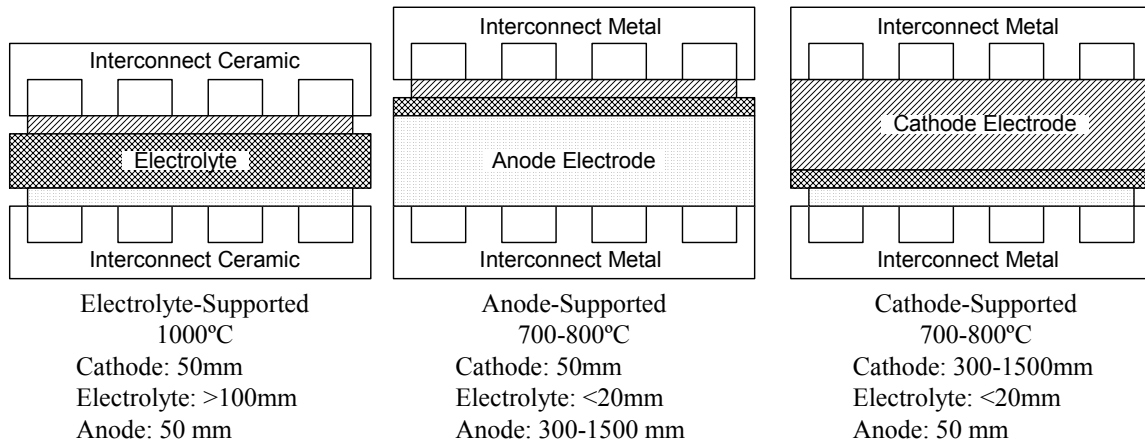

Electrolyte-Supported 1000ºC	Anode-Supported 700-800ºC	Cathode-Supported 700-800ºC
Cathode: 50mm	Cathode: 50mm	Cathode: 300-1500mm
Electrolyte: >100mm	Electrolyte: <20mm	Electrolyte: <20mm
Anode: 50 mm	Anode: 300-1500 mm	Anode: 50 mm

Figure 1 Planar Solid Oxide Fuel Cell (SOFC) Configurations

For optimal design and operation of SOFCs, a fundamental and detailed understanding of transport and electrochemical kinetics is necessary. Efforts are presently underway to understand the multi-physics and to obtain the optimal design for SOFC. For these purposes, a CFD-based model becomes a valuable tool for design and operation of SOFC.

In this paper, development of a multi-physics, electrochemical-transport coupled, and multi-dimensional SOFC model is described. The model is based on a single-domain modeling framework that has been successfully developed at ECEC for more complicated polymer electrolyte fuel cells (PEFC). The model involves solving conservation equations for mass, momentum, multi-component species, energy and electrical charge along with electrochemical kinetics in active regions of anode and cathode of a SOFC. In the following section, the model equations are provided and their implementation into the commercial CFD software Fluent[®] using User Defined Functions (UDF) is explained.

MODEL DEVELOPMENT

SOFC Basics

A schematic diagram of SOFC is given in Figure 2. A planar SOFC consists of anode gas channel, anode gas diffusion electrode, anode interlayer (active electrode), electrolyte, cathode interlayer (active electrode), cathode gas diffusion electrode and cathode gas channel. The electrochemical reactions are considered to occur at the active regions of the

porous electrodes (i.e. interlayer). In an SOFC, oxidant reduction occurs in the active cathode. The oxygen ion is then transported through the electrolyte and then in the active anode oxidation of the fuel occurs by the following reactions.

Oxidation of fuel at anode

$$H_2 + O^{2-} \rightarrow H_2O + 2e^- \qquad [1]$$

Reduction of oxidant at cathode

$$\frac{1}{2}O_2 + 2e^- \rightarrow O^{2-} \qquad [2]$$
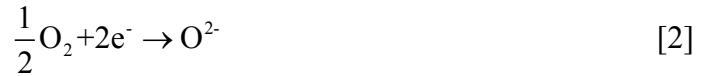
The anode is generally made of Nickel / Yttria – Stabilized Zirconia Cermet. The cathode is an LSM layer chemically expressed as $La_{1-x}Sr_xMnO_3$. The electrolyte is an Y_2O_3 doped ZrO_2 material called YSZ.
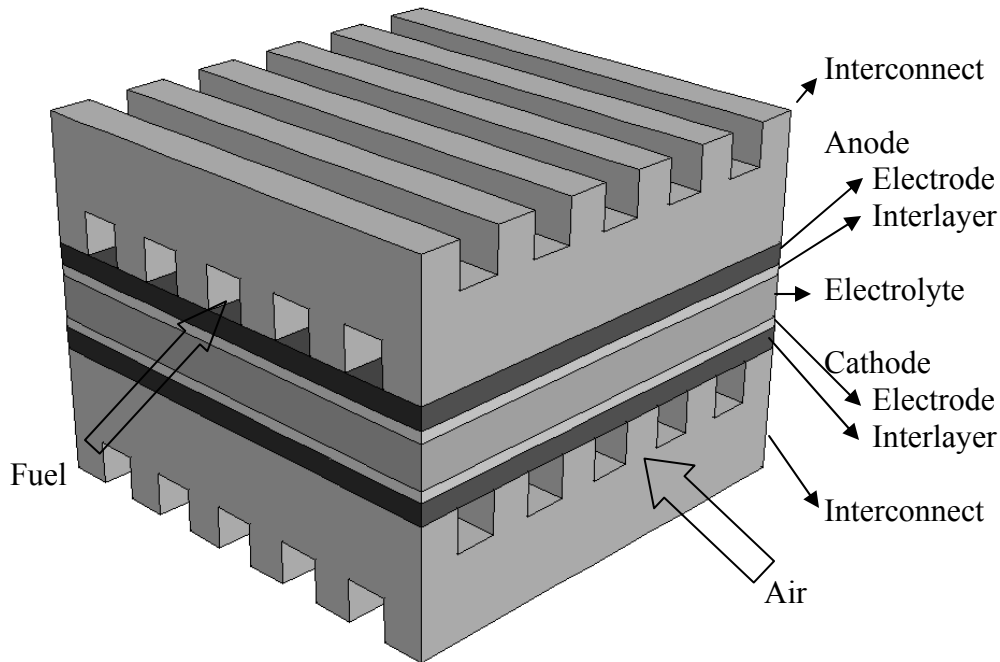

Figure 2 Planar SOFC Schematics

Model Equations

The governing equations for the SOFC model are summarized in Table 1. Although the model is fully transient in nature, sample results are provided only for steady state operation in this study. This model assumes *(i)* ideal gas mixtures; *(ii)* incompressible and laminar flow due to small pressure gradients and flow velocities; *(iii)* isotropic and homogeneous electrodes and *(iv)* negligible ohmic drop in electronically conductive solid matrix of porous electrodes as well as the current collectors.

The continuity and momentum equations determine the flow field throughout the entire cell. Within both porous electrodes, the generalized Darcy's law is employed.

The species transport equation is solved for three species: H_2, O_2 and H_2O, in sample calculations. However, the model is applicable to multiple fuels such as H_2 and CO given that kinetic expressions for co-oxidation of H_2 and CO on Ni catalysts are provided. N_2 is considered as an inert gas for this model.

Table 1 Governing Equations and Corresponding Source Terms

		Source terms		
	Conservation Equation	Porous Electrode	Active Electrode (interlayer)	Electrolyte
Mass	$\dfrac{\partial(\varepsilon\rho)}{\partial t}+\nabla\cdot(\rho\vec{u})=0$		$S_u=-\dfrac{\mu}{K}\vec{u}$	$\vec{u}=0$
N-S	$\dfrac{1}{\varepsilon}\left[\dfrac{\partial\rho\vec{u}}{\partial t}+\dfrac{1}{\varepsilon}\nabla\cdot(\rho\vec{u}\vec{u})\right]=-\nabla p+\nabla\cdot\tau+S_u$	$S_u=-\dfrac{\mu}{K}\vec{u}$	$S_u=-\dfrac{\mu}{K}\vec{u}$	$\vec{u}=0$
Species	$\dfrac{\partial(\varepsilon c_k)}{\partial t}+\nabla\cdot(\vec{u}c_k)=\nabla\cdot(D_k^{eff}\nabla c_k)+S_k$		$S_k=-\dfrac{s_k j}{n\ F}$	
Charge	$\nabla\cdot(\kappa^{eff}\nabla\Phi)+S_\Phi=0$		$S_\Phi=j$	
Heat	$\dfrac{\partial(\varepsilon\rho c_P T)}{\partial t}+\nabla\cdot(\rho c_P\vec{u}T)=\nabla\cdot(k^{eff}\nabla T)+S_T$		$S_T=\dfrac{i^2}{\kappa^{eff}}+$ $j\left(\eta+T\dfrac{dU_0}{dT}\right)$	$S_T=\dfrac{i^2}{\kappa^{eff}}$

The activation overpotential for both electrodes are relatively high; therefore the electrochemical kinetics of the both electrodes can be approximated by Tafel kinetics. Concentration dependence of exchange current density is given by Costamagna et al (2). That is, the resulting transfer current densities are:

$$j_a=\gamma_a\exp\left(-\frac{E_a}{RT}\right)\left(\frac{C_{H_2}}{C_{H_2 ref}}\right)\left(\frac{C_{H_2O}}{C_{H_2Oref}}\right)^{-\frac{1}{2}}\exp\left(\frac{\alpha_a F}{RT}\eta\right) \qquad [3]$$

at the anode and

$$j_c=-\gamma_c\exp\left(-\frac{E_c}{RT}\right)\left(\frac{C_{O_2}}{C_{O_2 ref}}\right)^{\frac{1}{4}}\exp\left(-\frac{\alpha_c F}{RT}\eta\right) \qquad [4]$$

at the cathode.

The kinetic parameters are given in Table 2 along with the requisite transport properties. The open circuit potential of a SOFC is calculated via the following Nernst equation (2):

$$V_{oc} = -\frac{\Delta G^o}{n_e F} - \frac{RT_s}{n_e F} \ln\left(\prod p_i^{v_i}\right)$$
[5]

The conductivity of the electrolyte, i.e. YSZ, is a strong function of temperature and increases with the temperature. The temperature dependence of the electrolyte conductivity is modeled by the Arrhenius equation i.e. (2)

$$\sigma T = A_o \exp\left(-\frac{E_o}{\kappa T}\right)$$
[6]

or
$$\sigma_{electrolyte} = \beta_1 \exp\left(-\frac{\beta_2}{T}\right)$$
[7]

Table 2 Electrochemical and Transport Properties

DESCRIPTION	UNIT	VALUE
Anode reference exchange current density (γ_a)	A/m^2	$1.67*10^8$
Cathode reference exchange current density (γ_c)	A/m^2	$5.51*10^9$
Anode Activation Energy (E$_a$) (2)	J/mol	$140*10^3$
Cathode Activation Energy (E$_c$) (2)	J/mol	$160*10^3$
Anode Transfer Coefficient (α_a) (2)		2
Cathode Transfer Coefficient (α_c) (2)		0.6
Electrolyte Conductive Coefficient (β_1) (2)	1/Ωm	$3.34*10^4$
Electrolyte Conductive Coefficient (β_2) (2)	K	$1.03*10^4$
Faraday Constant (F)	C/mol	96487
H$_2$ Diffusivity (2)	m^2/s	$3.5*10^{-5}$
O$_2$ Diffusivity (2)	m^2/s	$7.3*10^{-6}$
H$_2$O Diffusivity at Anode (2)	m^2/s	$3.5*10^{-5}$
H$_2$O Diffusivity at Cathode (2)	m^2/s	$7.3*10^{-6}$
Anode Viscosity	m^2/s	$2.89*10^{-5}$
Cathode Viscosity	m^2/s	$1.36*10^{-5}$
Material Properties		
Anode Electrode Porosity		0.5
Cathode Electrode Porosity		0.5
Permeability of Anode Electrode	m^2	$1.76*10^{-11}$
Permeability of Cathode Electrode	m^2	$1.76*10^{-11}$

NUMERICAL IMPLEMENTATION

For numerical testing and validation, both co-flow and cross-flow electrolyte-supported cells are considered. Cross-flow geometry is of particular interest because of the complex transport phenomena employed in this cell configuration and this configuration is able to provide detailed understanding of mass-transfer limitations. The dimensions of these

configurations are given in Table 3. Structured, orthogonal meshes are used for all computational meshing. We found that 80x80x35 mesh is sufficient for 3D, 5-channel geometry.

Appropriate source terms and diffusion coefficients are calculated by the customized user defined functions and then passed to the Fluent solver and resulting differential equations are solved by the solver.

The computation is assumed to be converged when the overall mass balance and species mass balances are met and the relative error between two consecutive iterations is less than 10^{-6}. It takes ~300 iterations and ~2.5 hours to solve the 3D 5-channel cross-flow geometry (i.e. 224, 000 cells).

RESULTS AND DISCUSSION

In Figure 4, the calculated current-voltage characteristic of the sample co-flow cell is given. The dimensions of this cell and operating conditions can be found in Table 3. The predicted polarization curve is in good qualitative agreement with published experimental data.
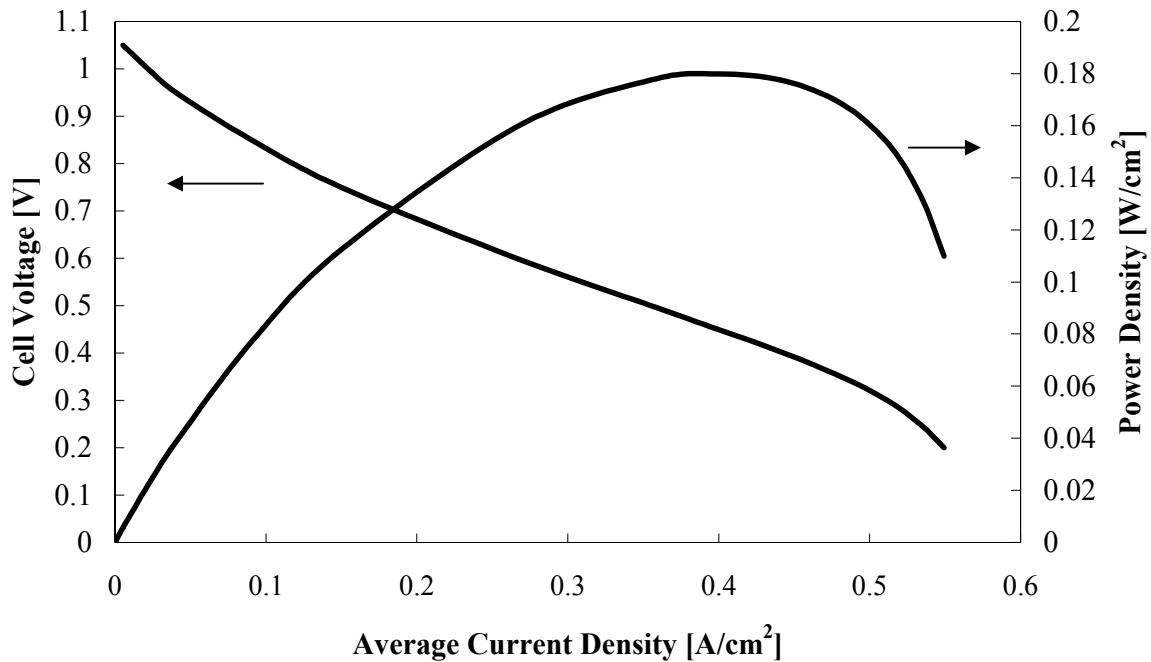

Figure 3 Calculated current-voltage characteristics and power density curve of electrolyte-supported co-flow SOFC. (Operating temperature 1000°C with anode and cathode stoichiometry of 1.5 and 2.0 @ 0.4 A/cm², respectively, other cell information is given in Table 3.

In addition to the current-voltage characteristics, the model is able to provide much more details on the transport and electrochemical processes occurring in SOFC. In Figure 4, the variation in the local current density along the channel direction at different cell voltages is provided. It is seen that at the cell voltage of 0.95 V, which is very close to the open circuit potential, the current density is almost uniform along the channel. This

shows that at this cell voltage, there are enough reactants for reaction throughout the cell; as a result, cell operation is not limited by mass transfer at any location of the cell. However, at lower cell voltages, it is seen that the current density is decreasing in the flow direction. It should be noted that the reactant species concentrations are also decreasing along the channel direction due to the electrochemical reaction at the active electrodes. Depletion of reactants results in the decrease of current density along the channel. Calculated reactant species concentration contours are displayed in Figure 5 for co-flow cells.

Table 3 Operating Conditions and Test Cell Dimensions

DESCRIPTION	UNIT	VALUE
Operating Conditions		
Reference Average Current Density	A/cm^2	0.4
Anode Stoichiometric Coefficient based on 0.4 A/cm^2		1.5
Cathode Stoichiometric Coefficient based on 0.4 A/cm^2		2.0
Anode Inlet Pressure	Atm	1.0
Cathode Inlet Pressure	Atm	1.0
Cell Temperature	℃	1000
Inlet Molar Concentrations		
Anode:		
Hydrogen	mol/m^3	8.616
Oxygen	mol/m^3	0
Water Vapor	mol/m^3	0.917
Cathode:		
Hydrogen	mol/m^3	0
Oxygen	mol/m^3	1.914
Water Vapor	mol/m^3	0.917
Test Cell Dimensions		
Cell Length	mm	16.0
Cell Height	mm	16.0
Current Collector Height	mm	1.0
Gas Channel Height	mm	2.0
Anode Gas Channel Width	mm	2.0
Cathode Gas Channel Width	mm	2.0
Anode Electrode Thickness	μm	50
Cathode Electrode Thickness	μm	50
Electrolyte Thickness	μm	180

In order to investigate the cross-flow transport characteristics in planar SOFC, a five-channel cross-flow type electrolyte-supported SOFC is simulated. The geometry and generated mesh for this cell is shown in Figure 6. It is clearly seen from the calculated current density distribution displayed in Figure 7, the regions facing the channels has much higher current density. This is clearly seen at the zones, where the corresponding anode and cathode channels meet. In those regions, both of the electrodes receive enough reactant, thereby producing higher current. This 3D calculation explicitly illustrates the effect of flow field design on cell performance.
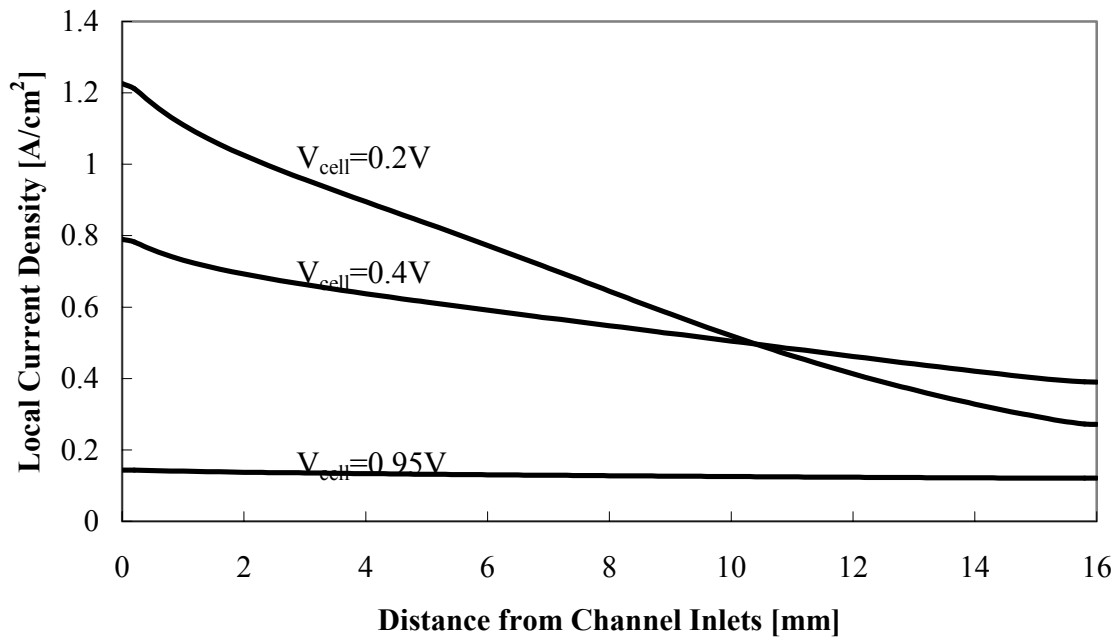
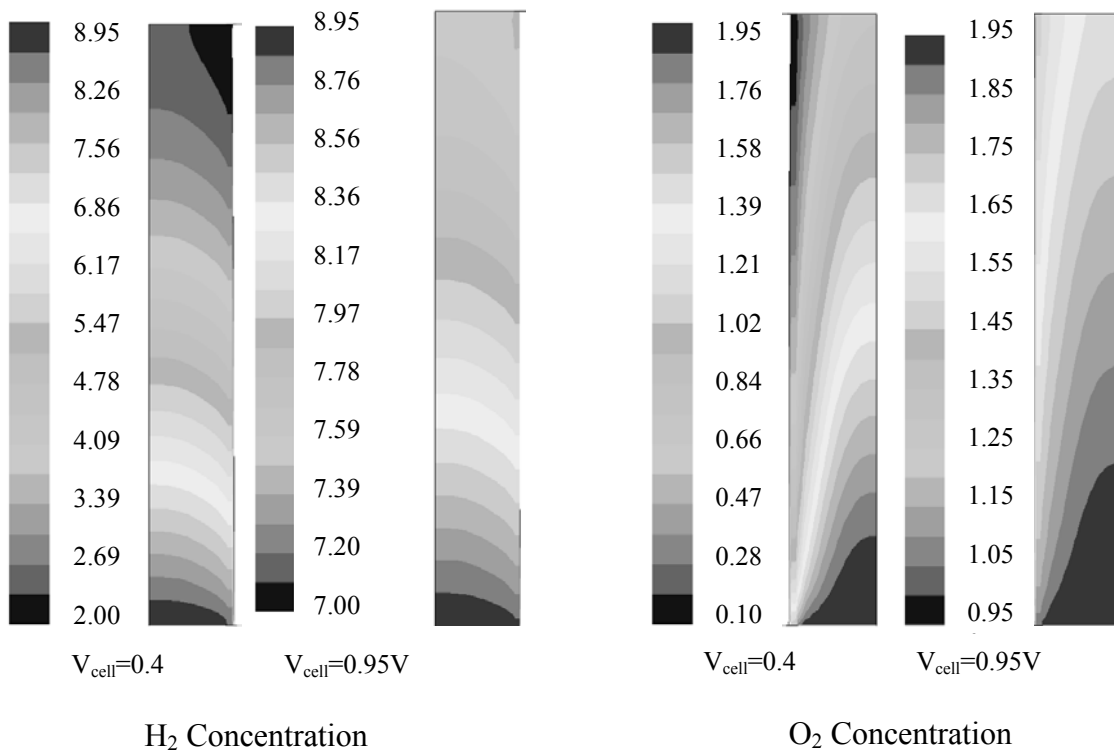**Figure 4 Calculated Current density distributions along the channel of co-flow SOFC at different cell voltages.**

H_2 Concentration

O_2 Concentration

Figure 5 Calculated Reactant Concentrations for Co-Flow Planar Electrolyte-Supported SOFC [mol/m^3]
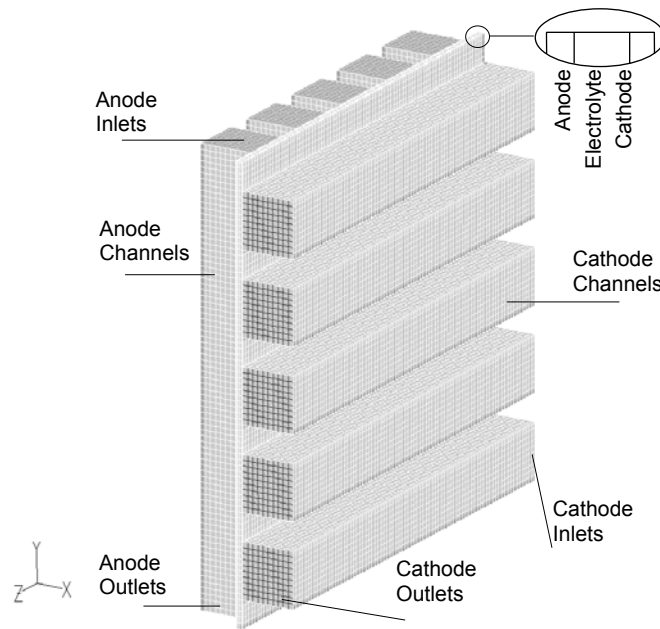
Figure 6 Geometry and Mesh of 5-channel Cross-Flow Electrolyte-Supported SOFC
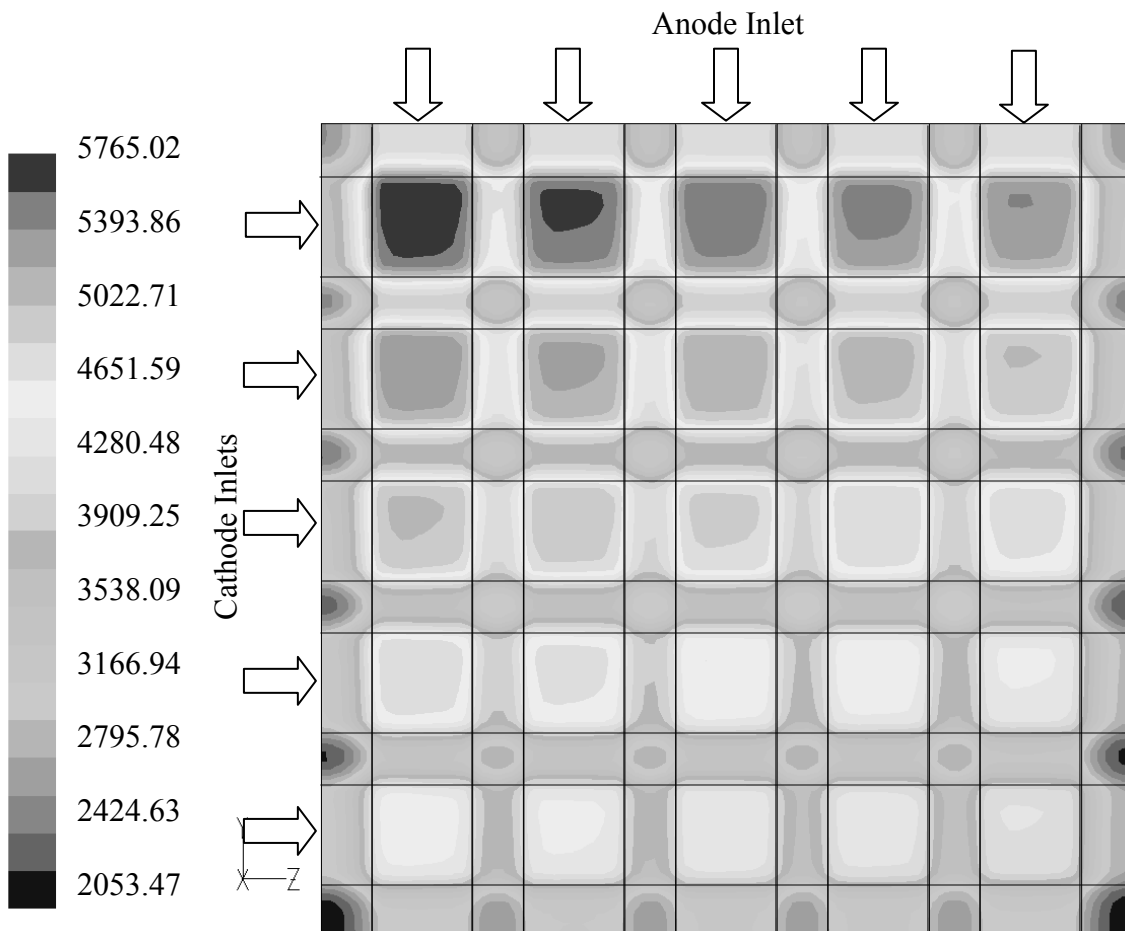

Figure 7 Current Density Distribution of 5-Channel Cross-Flow Electrolyte Supported SOFC [A/m^2] (Anode and Cathode Stoichiometry, 1.5 and 2.0, respectively, Operating Temperature, 1000ºC, Cell Voltage 0.4V)

CONCLUSIONS AND FUTURE WORK

A single-domain formulation was developed to comprehensively describe the electrochemistry, hydrodynamics and multi-component transport of SOFC. The model was implemented into the commercial CFD software Fluent. The CFD model was shown to be able to predict the current-voltage characteristics of SOFC, in addition to the detailed reactant and product distributions in the cell. This data makes it possible to analyze SOFC operation in detail.

The CFD model described in this study is intended to present a tool for design optimization of SOFCs. To achieve this and fully utilize this tool, the model can be used to perform parametric and sensitivity studies of varying operating conditions and cell designs.

The present CFD model also has the energy equation built in to resolve the temperature distribution (not shown due to trivialness for a small single cell). However, a detailed account of various heat generating sources such as irreversible and reversible (entropic) heat as well as ohmic heating has been provided. The temperature distribution can be used to couple to stress analyses, thereby providing a comprehensive computer-aided engineering (CAE) tool for SOFC design and operation.

The present model can be easily extended to include multiple fuels such as H_2 and CO. In such a case, co-oxidation of H_2 and CO on Ni catalyst must be considered following a similar approach already developed for PEFC in the presence of CO poisoning (Ju et al. 2002). Finally, the present model serves as a building block to build a comprehensive CFD-based model for SOFC with internal reforming on the anode. In such a situation, catalytic chemical reaction is additionally needed in the present model.

REFERENCES

1. H.Yakabe, T. Ogiwara, M. Hishinuma and I. Yasuda, *J. Power Sources,* **102** 144 (2001)

2. P. Costamagna and K. Honegger, *J. Electrochem. Soc.,* **145**, 3995 (1998).

3. S. C. Singhal, *presented in INDO-US Fuel Cell Workshop*, Washington, DC (2002).

4. A. M. Svensson and K. Nisancioglu, *J. Electrochem. Soc.* **145**, 3130 (1998).

5. S. Ahmed, C. McPheeters and R. Kumar, *J. Electrochem. Soc.,* **138**, 2712 (1991),

6. N. F. Bessette II, W .J. Wepfer and J. Winnick, *J. Electrochem. Soc.,* **142**, 3792 (1995).